Chemico-Biological Interactions 184 (2010) 439–448

Contents lists available at ScienceDirect

Chemico-Biological Interactions

journal homepage: www.elsevier.com/locate/chembioint

Cytotoxic activity of naphthoquinones with special emphasis on juglone and its 5-*O*-methyl derivative

Raquel Carvalho Montenegro[a,*], Ana Jérsia Araújo[a], María Teresa Molina[b], José Delano Barreto Marinho Filho[a], Danilo Damasceno Rocha[a], Eulogio Lopéz-Montero[b], Marília O.F. Goulart[c], E.S. Bento[c], Ana Paula Nunes Negreiros Alves[d], Cláudia Pessoa[a], Manoel Odorico de Moraes[a], Letícia Veras Costa-Lotufo[a]

[a] *Departamento de Fisiologia e Farmacologia, Universidade Federal do Ceará, Campus do Porangabussu, Caixa Postal 3157, Fortaleza, Ceará, 60430-270, Brazil*
[b] *Instituto de Química Médica – Consejo Superior de Investigaciones Científicas (CSIC), 28006 Madrid, Spain*
[c] *Instituto de Química e Biotecnologia, Universidade Federal de Alagoas, Tabuleiro do Martins, Maceió, Alagoas, 57072-970, Brazil*
[d] *Departamento de Odontologia Clínica, Universidade Federal de Ceará, Fortaleza, Ceará, Brazil*

ARTICLE INFO

Article history:
Received 21 November 2009
Received in revised form 26 January 2010
Accepted 27 January 2010
Available online 4 February 2010

Keywords:
Naphthoquinones
Juglone
Cytotoxicity
Apoptosis
Caspases
Cell cycle

ABSTRACT

The cytotoxicity of nine naphthoquinones (NQ) was assayed against HL-60 (leukaemia), MDA-MB-435 (melanoma), SF-295 (brain) and HCT-8 (colon), all human cancer cell lines, and peripheral blood mononuclear cells (PBMC), as representatives of normal cells, after 72 h of incubation. 5-Methoxy-1,4-naphthoquinone was the most active compound, showing IC_{50} values in the range of 0.31 (1.7 μM) in HL-60 to 0.88 μg/mL (4.7 μM) in SF-295 and IC_{50} of 0.69 μg/mL (3.7 μM) against PBMC. With the introduction of a bromo-substituent in position 2 or 3 of juglone, the IC_{50} significantly decreased, regardless of the position on the NQ moiety. However, compared with juglone methyl ether, the halogen substitution decreased the activity. To further understand the mechanism underlying the cytotoxicity of 5-methoxy-1,4-naphthoquinone, studies involving DNA fragmentation, cell cycle analysis, phosphatidyl serine externalization, mitochondrial depolarization and activation of caspases 8 and 3/7 were performed in HL-60 cell line, using doxorubicin as a positive control. The results indicate that the cytotoxic 5-methoxy-1,4-naphthoquinone activates caspases 8 and 3/7 and thus induces apoptosis independent of mitochondria.

1. Introduction

Quinones still account for one of the largest families of antitumor agents. Although most current anticancer drugs were discovered empirically, considerable insight has been gained into the mechanisms by which many of these compounds affect cellular growth [1–3]. The basic knowledge on quinone studies has been used to design new anticancer drugs [4–6], improving selectivity and providing a more rational therapeutic application of these agents.

Juglone (5-hydroxy-1,4-naphthoquinone) is a natural 1,4-naphthoquinone found in the Juglandaceae family, particularly in the roots, leaves, bark and wood of *Juglans regia* (English walnut, Persian walnut and California walnut), *J. cinerea* (butternut and white walnut), and *J. nigra* (black walnut). Juglone has shown cytotoxic effects against various tumor cells [7–11] and also has antifungal, antibacterial and antiviral activities, as well as allelophatic activities [12]. Sugie et al. [13] found that juglone reduced the formation of azoxymethane induced intestinal tumors in F344 rats and concluded that juglone could be a promising chemopreventive agent. Several proposals have been made to explain the mode of action underlying cytotoxicity of juglone [9,11]. Although this molecule has multiple effects, including apoptosis [9,14,15], it is well known that these effects are cell-type-specific [14] and the exact mechanism remains unclear. Very recently, Aithal et al. [16] demonstrated cytotoxic and genotoxic potentials of juglone, which can be attributed to mechanisms including the induction of oxidative stress, cell membrane damage, and a clastogenic action leading to cell death by both apoptosis and necrosis.

Bromo-juglone derivatives are very useful from the synthetic standpoint because they have been used as synthons for the regioselective preparation of anthraquinones [17], angucyclines [18] and benz[b]phenantridines [19], among other classes of natural products. To the best of our knowledge, so far, only one recent study on their biological properties has been published [20].

* Corresponding author at: Departamento de Fisiologia e Farmacologia, Universidade Federal do Ceará, Rua Cel. Nunes de Melo, 1127, P.O. Box 3157, 60430-270 Fortaleza, CE, Brazil. Tel.: +55 85 3366 8255; fax: +55 85 3366 8333.
E-mail address: rc_montenegro@yahoo.com.br (R.C. Montenegro).

0009-2797/$ – see front matter © 2010 Elsevier Ireland Ltd. All rights reserved.
doi:10.1016/j.cbi.2010.01.041

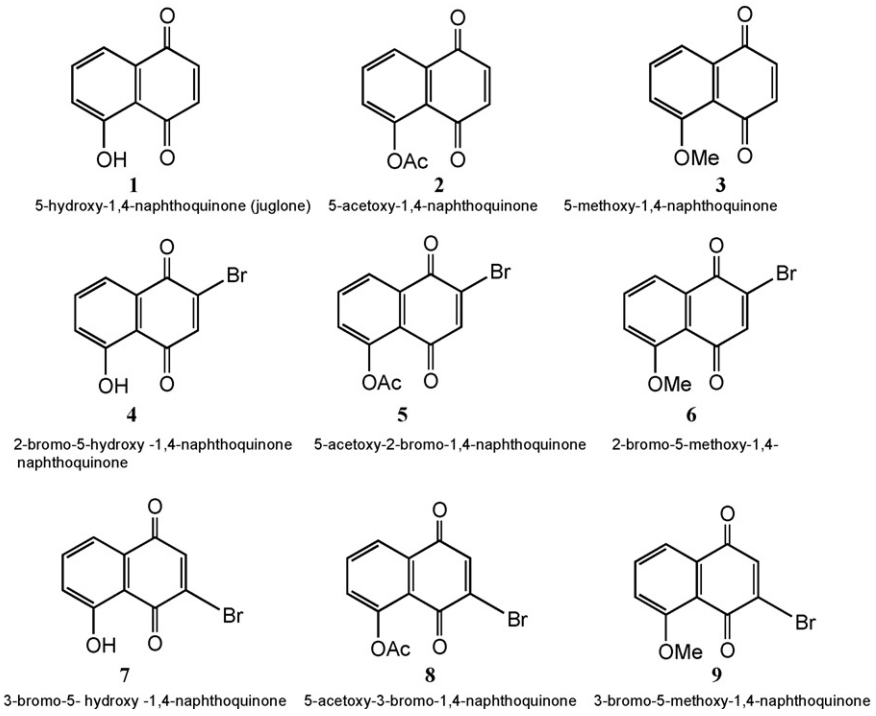

Fig. 1. Chemical structures of juglone (**1**) and its derivatives (**2–9**).

In the search for new quinone-derived anticancer compounds, in this paper, the cytotoxic effects of juglone (**1**) and some derivatives (**2–9**) (Fig. 1) toward four tumor cell lines are reported, using the anthraquinone doxorubicin as a positive control (Table 1). Also, in a second set of experiments, the effects of the most active derivative, 5-methoxy-1,4-naphthoquinone (**3**), were assessed using HL-60 cell line and then compared to juglone (**1**). To further understand the mechanism underlying the cytotoxicity of compound **3**, studies involving DNA fragmentation, cell cycle analysis, phosphatidyl serine externalization and mitochondrial depolarization were performed. In search for selectivity, the cytotoxicity of compounds **1** and **3** was also evaluated in human peripheral blood mononuclear cells (PBMC) (Table 1).

Table 1
Cytotoxic activity of juglone and its derivatives on tumor cell lines, on peripheral blood mononuclear cells and erythrocytes.

	MTT IC_{50} μg/mL (μM)*					Hemolysis EC_{50} (μg/mL)
	HL-60	MDAMB 435	SF-295	HCT-8	PBMC	
1	>5 (28.7)	>5 (28.7)	2.97 (17.0) 2.01–4.38	1.33 (7.6) 0.74–2.39	>5 (28.7)	>200
2	1.98 (9.2) 1.69–2.33	1.35 (6.2) 1.03–1.77	1.82 (8.4) 1.6–2.07	1.11 (5.1) 0.77–1.6	nd	>200
3	0.31 (1.7) 0.23–0.43	0.72 (3.8) 0.62–0.95	0.88 (4.7) 0.72–1.07	0.85 (4.5) 0.71–1.05	0.69 (3.7) 0.49–0.99	>200
4	1.08 (4.3) 0.93–1.23	1.39 (5.5) 1.06–1.82	1.6 (6.3) 1.29–1.99	1.62 (6.4) 1.12–2.35	nd	>200
5	2.31 (7.8) 1.86–2.89	1.85 (6.3) 1.37–2.5	1.81 (6.1) 1.47–2.23	1.58 (5.3) 1.32–1.86	nd	>200
6	2.99 (11.2) 2.4–3.7	2.36 (8.8) 1.84–3.03	2.2 (8.2) 1.02–4.71	2.35 (8.8) 1.59–3.46	nd	>200
7	1.52 (6.0) 1.04–2.25	2.26 (8.9) 1.48–3.42	2.92 (11.5) 2.31–3.69	2.23 (8.8) 1.78–2.79	nd	>200
8	2.33 (7.9) 1.79–3.04	2.48 (8.4) 1.84–3.35	2.30 (8.6) 1.82–2.91	2.61 (7.8) 1.81–3.77	nd	>200
9	1.93 (7.2) 1.54–2.42	1.73 (6.5) 1.38–2.16	1.41 (5.3) 1.18–1.67	1.54 (5.8) 1.08–2.19	nd	>200
Dox	0.02 (0.03) 0.01–0.02	0.48 (0.8) 0.34–0.66	0.23 (0.4) 0.19–0.25	0.01 (0.02) 0.01–0.02	0.97 (1.7) 0.52–1.80	nd

* Data are presented as IC_{50} values and 95% of confidence interval for leukaemia (HL-60), melanoma (MDAMB-435), nervous system (SF-295), colon (HCT-8) cancer cells and peripheral blood mononuclear cells (PBMC). Doxorubicin (Dox) was used as a positive control. Experiments were performed in triplicate. nd – not determined.

2. Materials and methods

Melting points were measured with a Reichert-Jung Kofler hot-stage microscope and are uncorrected. Infrared spectra were recorded with a Shimadzu IR-435 and the ^{1}H and ^{13}C NMR spectra with Varian Gemini 200 (200 MHz), Bruker 300 (300 MHz), Varian Inova 400 (400 MHz) and/or Bruker Avance 400 (400 MHz) spectrometers. Chemical shifts are reported in ppm on the delta scale, using chloroform-d as internal standard, and coupling constants (J) are given in Hz. Data processing was performed off-line with the TOPSPIN (Bruker) program package. Mass spectra (electronic impact) were recorded with a Hewlett-Packard 5973 MSD instrument.

2.1. Synthesis of juglone derivatives

All the naphthoquinone derivatives **1–9** used in this study are known compounds and were prepared according to the methods described in the literature.

Juglone (**1**) is a commercial material (Sigma–Aldrich, St. Louis, USA) and, when needed in large scale, was prepared according to the method by Tietze [21] and was purified by flash chromatography (chloroform). The spectroscopic data are compatible with those already reported [21]. Orange-red needles; 154–162 °C, lit. [21] 154–161 °C. IR (KBr) ν: 3062, 1665 (free C=O), 1643 (chelated C=O), 1600, 1451, 1363, 1337, 1290 (C–O), 1225. ^{1}H NMR (400 MHz, $CDCl_3$): δ 6.96 (s, 2 H, 2-H, 3-H), 7.29 (dd, J = 6.3, J = 2.9 Hz, 1 H, 6-H), 7.64 (m, 2 H, 7-H, 8-H), 12.01 (s, 1 H, OH) ppm. ^{13}C NMR (100 MHz, $CDCl_3$): δ 114.92 (C-4a), 119.13 (C-6), 124.47 (C-8), 131.70 (C-8a), 138.62 (C-7), 136.54, 139.56 (C-2, C-3), 161.40 (C-5), 184.22, 190.25 (C-1, C-4) ppm. EI-MS m/z (%) 174.1 (M^+,100), 158.1 (4), 146.1 (8), 118.1 (22), 92.0 (16), 63.0 (10) [21].

2.1.1. 5-Acetoxy-1,4-naphthoquinone (**2**)

Yellow prisms; mp 145–151 °C, lit., mp 150–151 °C [22]; mp 153–154 °C [23]. Acetylation of juglone under standard conditions afforded juglone acetate (**2**) [23]. IR (KBr) ν: 1758 (ester), 1662, 1610,1594, 1444, 1367, 1331, 1296, 1274. ^{1}H NMR (400 MHz, $CDCl_3$): δ 2.46 (s, 3 H, $-CH_3$), 6.88 (d, J = 10.26 Hz, 1 H, H-3), 6.95 (d, J = 10.26 Hz, 1 H, H-2), 7.41 (dd, J = 7.78, J = 1.26, 1 H, H-6), 7.78 (t, J = 7.78, 1 H, H-7), 8.07 (dd, J = 7.78, J = 1.26, 1 H, H-8). ^{13}C NMR (100 MHz, $CDCl_3$): δ 21.30 ($CO\underline{C}H_3$), 124.27 (C-4a), 125.23 (C-8), 129.98 (C-6), 133.78 (C-8a), 135.09 (C-7), 137.58 (C-2), 140.13 (C-3), 149.79 (C-5), 169.68 ($\underline{C}OCH_3$), 183.89 (C-4), 184.43 (C-1). EI-MS m/z (%) 216 (M^+, 6); 174 (100); 146 (7); 118 (12); 92 (7). Mass spectrum was similar to the one reported by Bowie et al. [24].

2.1.2. 5-Methoxy-1,4-naphthoquinone (**3**)

Bright yellow prisms; mp 186–190 °C (lit. mp 182–185 °C [23]; 184–189 °C [21]) was prepared by methylation of juglone (methyl iodide, silver (I) oxide) [21,23,26]. IR (KBr) ν: 1655 (C=O), 1614, 1583, 1470, 1443, 1377, 1336, 1298 (C–O), 1275, 1253. ^{1}H NMR (400 MHz, $CDCl_3$): δ 4.02 (s, 3 H, $-OCH_3$), 6.88 (s, 2 H, H-2, H-3), 7.33 (dd, J = 8.01, J = 1.28 Hz, 1 H, H-6), 7.70 (t, J = 8.01, 1 H, H-7), 7.75 (dd, J = 8.01, J = 1.28 Hz, 1 H, H-8), ^{13}C NMR (100 MHz, $CDCl_3$): δ 56.70 ($O\underline{C}H_3$), 118.14 (C-6), 119.15 (C-8), 119.58 (C-4A), 134.25 (C-8A), 135.22 (C-7), 136.43 (C-2), 141.11 (C-3), 159.84 (C-9), 184.59 (C-4), 185.44 (C-1). EI-MS m/z (%): 188.1 (M^+,100), 174.1 (20), 159.1 (18), 130 (16), 104 (18), 76 (20), 63 (12). Mass spectrum corresponds to data reported by Bowie et al. [24].

2.1.3. 2-Bromo-5-hydroxy-1,4-naphthoquinone (**4**)

Orange needles; mp 130–135 °C, lit. 135–136 °C [27] was prepared according to reported procedure by hydrolysis of the corresponding acetate **5** [27]. The data are compatible to those already reported [27,28]. IR (KBr) ν: 1683, 1644, 1590, 1460, 1365, 1308, 1255, 1176, 1097, 905, 815 cm^{-1}. EI-MS m/z (%): 254 (M′, 100.0), 252 (M′, 98.1), 173 (90.31, 145 (44.1), 89 (35.5), 63 (54.0), 62 (22.2), 53 (29.1) [28]. ^{1}H NMR (400 MHz, $CDCl_3$): δ 7.32 (dd, J = 8.3, J = 1.4, 1 H, H-6), 7.50 (s, 1 H, H-3), 7.64 (dd, J = 8.3, J = 7.4, 1 H, H-7), 7.75 (dd, J = 7.4, J = 1.4, 1 H, 8-H), 11.77 (s, 1 H, OH), ^{13}C NMR (100 MHz, $CDCl_3$): δ 114.6 (C-4a), 121.0 (C-8), 125.1 (C-6), 130.7 (C-8a), 136.4 (C-7), 140.3 (C-3), 140.9 (C-2), 161.7 (C-5), 176.0 (C-1), 187.5 (C-4).

2.1.4. 5-Acetoxy-2-bromo-1,4-naphthoquinone (**5**)

Yellow needles mp 159–161 °C, lit. 155–156 °C [27]. Obtained from **4** by standard acetylation [29,30]. IR (KBr) ν: 1682,1600,1370,1330,1270,1190, 1098, EI-MS m/z (%): 296 (1.7). (M^+), 294 (0.8) (M^+), 254 (70.9), 252 (67.5), 173 (35.5), 145 (10.6), 63 (12.9), 43 (100.0). Data are compatible with those already published [27].

2.1.5. 2-Bromo-5-methoxy-1,4-naphthoquinone (**6**)

Yellow needles, mp 127–130 °C, lit.132–133 °C [31] were synthesized by standard methylation of **4** that led to the corresponding methyl ether **6** [31,32]. IR (KBr) ν: 2975, 1680, 1650, 1595,1475,1458,1293,1245,1120, 1042, 908, 813 cm^{-1}. EI-MS m/z (%): 268 (100.0) (M^+), 266 (98.0) (M^+), 187 (35.9), 159 (24.9), 157 (43.5), 131 (27.4), 129 (40.9), 116 (37.9), 101 (31.2), 76 (33.0), 75 (28.0), 74 (25.2), 63 (23.2), 62 (31.6), 53 (23.7). ^{1}H NMR (400 MHz, $CDCl_3$): δ 4.03 (s, 3 H, OCH_3), 7.36 (dd, J = 7.68, J = 1.13, 1 H, H-6), 7.42 (s, 1 H, H-3), 7.71 (t, J = 7.68, H-7), 7.85 (dd, J = 7.68, J = 113, 1 H, H-8), ^{13}C NMR (100 MHz, $CDCl_3$): δ 56.81 ($O\underline{C}H_3$) 118.49 (C-6), 118.67 (C-4a), 120.88 (C-8), 135.08 (C-7), 135.34 (C-8a), 137.11 (C-2), 142.54 (C-3), 160.24 (C-5), 178.54 (C-4), 182.78 (C-1).

The 3-bromo-juglone derivatives were prepared by selective bromination of juglone according to Brimble [28], which yielded **7** as the major isomer.

2.1.6. 3-Bromo-5-hydroxy-1,4-naphthoquinone (**7**)

Dark red needles; mp 171–174 °C, lit. mp 172 °C [27]. Data are compatible to those reported [27,28].

2.1.7. 5-Acetoxy-3-bromo-1,4-naphthoquinone (**8**)

Yellow needles, mp 145–149 °C, lit. 149–150 [27] obtained from **7** by standard acetylation [29,30]. Data match those already published [27]. EI-MS m/z (%): 253.9, 251.9 (42,40), 173.0 (32), 145.0 (30), 95.1 (22), 81.1 (53), 69.1 (100), 57.1 (52). ^{1}H NMR (400 MHz, $CDCl_3$): δ 2.45 (s, 3 H, $-CO\underline{C}H_3$), 7.42 (dd, J = 8, J = 1.5, 1 H), 7.53 (s, 1 H, H-2), 7.75 (t, J = 8, 1 H, H-7), 8.01 (dd, J = 8, J = 1.5, 1 H, H-8). ^{13}C NMR (100 MHz, $CDCl_3$): δ 20.9 ($CO\underline{C}H_3$), 122.9 (s), 125.4 (d), 130.3 (d), 133.9 (s), 135.7 (d), 139.5 (d), 141.2 (s), 150.9 (s), 169.3 (s), 176.3 (s), 181.6 (s).

2.1.8. 3-Bromo-5-methoxy-1,4-naphthoquinone (**9**)

Yellow needles, mp 150–153 °C, lit. 154–155 °C [25,33], obtained from **7** by standard methylation (methyl iodide, silver (I) oxide) [33]. IR (KBr) ν: 3043, 1673,1652,1581, 1470, 1444, 1336, 1311, 1276, 1212. ^{1}H NMR (400 MHz, $CDCl_3$): δ 4.04 (s, 3 H, $-OCH_3$), 7.34 (dd, J = 2.37, J = 7.25, 1 H, H-6), 7.46 (s, 1 H, H-2), 7.72 (t, J = 7.25, H-7), 7.75 (m, 1 H H-8). ^{13}C NMR (100 MHz, $CDCl_3$): δ 56.78 (OCH_3), 118.31 (C-4a), 118,31 (C-6), 119,73 (C-8), 133.74 (C-8a), 135.80 (C-7), 138.56 (C-2), 142.84 (C-3), 160.65 (C-5), 176.20 (C-4), 182.87 (C-1). The spectral data are in agreement with those already published [33].

Compounds **1**–**3** and several bromo-derivatives were recently used as starting materials for the synthesis of benzo-fused 1,4-quinones [34].

Each compound was dissolved in DMSO to obtain a concentration of 5 mg/mL. For the experiments, the vehicle concentration, DMSO, was kept at a maximum of 0.1%.

2.2. Cell line and cell culture

The tumor cell lines used in this work were HL-60 (leukaemia), HCT-8 (colon carcinoma), MDA-MB 435 (melanoma) and SF-295 (nervous system) kindly provided by the National Cancer Institute (Bethesda, MD, USA). Also, peripheral blood mononuclear cells (PBMC) were tested, for chosen compounds. Heparinized blood (from healthy, non-smoker donors who had not taken any drug at least 15 days prior to sampling) was collected and PBMC were isolated by a standard method of density-gradient centrifugation over Ficoll-Hypaque. PBMC were washed and resuspended at a concentration of 3×10^5 cells/mL and platted in a 96-well plate with RPMI 1640 medium supplemented with 20% fetal bovine serum, 2 mM glutamine, 100 U/mL penicillin, 100 μg/mL streptomycin at 37 °C with 5% CO_2. Phytohemagglutinin (3%) was added at the beginning of culture. After 24 h, the compound (0.01–10 μM) dissolved in DMSO 1% was added to each well and incubated for 72 h. All cancer cells were maintained in RPMI 1640 medium supplemented with 10% fetal bovine serum, 2 mM glutamine, 100 U/mL penicillin, 100 μg/mL streptomycin at 37 °C with 5% CO_2.

2.3. MTT assay

The cytotoxicity of all compounds was tested against four tumor cell lines using the 3-(4,5-dimethyl-2-thiazolyl)-2,5-diphenyl-*2H*-tetrazolium bromide (MTT) (Sigma Aldrich Co., St. Louis, MO/USA) reduction assay [35]. For all experiments, cells were plated in 96-well plates (10^5 cells/well for adherent cells or 3×10^5 cells/well for suspended cells in 100 μL of medium). Compounds **1–9** (0.01–5 μg/mL) dissolved in DMSO 1% were added to each well (using the HTS – high-throughput screening – biomek 3000 – Beckman Coulter, Inc. Fullerton, California, USA) and incubated for 72 h. Control groups received the same amount of DMSO. After 69 h of incubation, the supernatant was replaced by fresh medium containing MTT (0.5 mg/mL). Three hours later, the MTT formazan product was dissolved in 150 μL of DMSO, and absorbance was measured at 595 nm (DTX 880 Multimode Detector, Beckman Coulter, Inc. Fullerton, CA, USA). Doxorubicin (0.01–5 μg/mL) was used as positive control.

2.4. Alamar Blue assay

In order to investigate the selectivity of compounds **1** and **3** toward a normal proliferating cell, the Alamar Blue assay was performed with peripheral blood mononuclear cells (PBMC) after 72 h drug exposure [36]. Briefly, PBMC were plated in 96-well plates (2×10^4 cells/well in 100 μL of medium). After 24 h, compounds **1** and **3** (0.01–25 μg/mL) dissolved in DMSO 1% were added to each well using the HTS and incubated for 72 h. Doxorubicin (0.009–5 μg/mL) was used as a positive control. Control groups received the same amount of DMSO. Twenty-four hours before the end of incubation, 10 μL of stock solution (0.436 mg/mL) of the Alamar Blue (resazurin – Sigma Aldrich Co., St. Louis, MO/USA) was added to each well. The absorbance was measured using a multiplate reader (DTX 880 Multimode Detector, Beckman Coulter, Inc. Fullerton, California, USA). The drug effect was quantified as the percentage of control absorbance at 570 and 595 nm [36].

2.5. Analysis of possible mechanisms involved in the cytotoxic activity of 5-methoxy-1,4-naphthoquinone

In order to study the mechanism involved in the activity of **1** and **3**, a second set of experiments was performed, where leukaemia cells (HL-60 cell line) were incubated, for 24 h, with the tested compounds (**1** and **3**). Compound **1** was tested at 4 μM and compound **3** at 0.5, 1.0, 2.0, 4.0, 8.0 and 10 μM. In these experiments, doxorubicin (0.5 μM) was used as a positive control.

2.5.1. Analysis of morphological changes

Untreated and treated HL-60 cells were examined for morphological changes by light microscopy (Olympus, Tokyo, Japan). To evaluate cell morphology, cells were harvested, transferred to cytospin slides, fixed with methanol for 1 min and stained with hematoxylin and eosin (HE) (Doles, Brazil). To evaluate nuclear morphology, HL-60 cells were stained with May-Grunwald-Giemsa (Bioclin, Brazil).

2.5.2. Acridine orange/ethidium bromide assay to determine cell death

Cell death pattern was determined by differential staining with acridine orange/ethidium bromide (AO/BE) (Sigma–Aldrich). Briefly, cells were pelleted and resuspended in 25 μL in PBS. Afterwards, 1 μL of aqueous solution of acridine orange/ethidium bromide (AO/EB, 100 μg/mL) was added and the cells were observed under a fluorescence microscope (Olympus, Tokyo, Japan). Three hundred cells were analyzed using a fluorescence microscope with filter for 470/40 nm. The cells were then classified as follows: live cells, apoptotic cells and necrotic cells. The percentage of apoptotic and necrotic cells was then calculated as described [37].

2.5.3. Flow cytometry analysis

For all tested compounds, five thousand events were evaluated per experiment and cellular debris was omitted from the analysis. HL-60 cell fluorescence was then determined by flow cytometry in a Guava EasyCyte Mine using Guava Express Plus software. Internucleosomal DNA fragmentation and cell cycle were analyzed by ModFit LT for Win32 version 3.1.

2.5.3.1. Cell membrane integrity. The cell membrane integrity was evaluated by the exclusion of propidium iodide (50 μg/mL, Sigma Aldrich Co., St. Louis, MO/USA). Briefly, 100 μL of treated and untreated cells were incubated with propidium iodide (50 μg/mL). The cells were, then, incubated for 5 min. Fluorescence was measured and analyzed for cell morphology, granularity and membrane integrity [38].

2.5.3.2. Internucleosomal DNA fragmentation and cell cycle analysis. DNA fragmentation was analyzed by flow cytometry after DNA staining with propidium iodide. Briefly, 100 μL of treated and untreated cells were incubated for 30 min, in the dark, with hypotonic solution containing 50 μg/mL propidium iodide, 0.1% sodium citrate, and 0.1% Triton X-100. Fluorescence was measured and DNA fragmentation and cell cycle were analyzed [39].

2.5.3.3. Phosphatidylserine (PS) externalization. PS externalization was analyzed by flow cytometry after PS staining with Annexin V according to the method described by Vermes et al. [40]. Guava Nexin Assay Kit was used to determine early apoptosis. Cells were washed twice with cold PBS and then resuspended in 135 μL of PBS with 5 μL of 7-amino-actinomycin D (7AAD) and 10 μL of Annexin V-PE. The cells were gently vortexed and incubated for 20 min at room temperature (20–25 °C) in the dark. Afterwards, the cells were analyzed by flow cytometry (EasyCyte from Guava Technologies). Annexin V is a phospholipid-binding protein that has a high affinity for PS. 7-AAD, a cell impermeant dye, is used as an indicator of membrane structural integrity. Fluorescence of Annexin V-PE was measured: yellow fluorescence-583 nm and 7-AAD in red fluorescence-680 nm. The percentage of

early and late apoptotic cells and necrotic cells was then calculated.

2.5.3.4. Mitochondrial transmembrane potential. Mitochondrial depolarization was evaluated by incorporation of Rhodamine 123 (Sigma Aldrich Co., St. Louis, MO/USA). Rhodamine 123 is a cell-permeable, cationic, fluorescent dye that is readily sequestered by active mitochondria without inducing cytotoxic effects. Briefly, cells were centrifuged at 2000 rpm for 5 min and the pellet was resuspended in 500 μL of 1 μg/mL of rhodamine 123 for 15 min in the dark. After incubation, cells were centrifuged at 2000 rpm for 5 min and the pellet was resuspended in 500 μL in phosphate-buffered saline (PBS) and incubated for 30 min in the dark. Fluorescence was measured and percentage mitochondrial depolarization was analyzed [37].

2.5.3.5. Caspases activity. Caspase 3/7 and 8 activities were analyzed by flow cytometry, using Guava® EasyCyte Caspase Kit, after 24 h of incubation. HL-60 cells (3×10^5 cells/mL) were incubated with Fluorescent Labeled Inhibitor of Caspases (FLICA) and maintained for 1 h at 37 °C and 5% CO_2. After incubation, 80 μL of washing buffer were added and cells were centrifuged at 2000 rpm for 5 min. The resulting pellet was resuspended in 200 μL of washing buffer and centrifuged again. Then the cells were resuspended in the working solution (propidium iodide 1:200 in 1× washing buffer) and analyzed immediately using flow cytometry.

2.5.4. Statistical analysis

Data obtained from experiments are presented as means ± SEM from at least three independent experiments and evaluated by Newman–Keuls test and the significance level was also set at 1%.

3. Results

3.1. Cytotoxicity of juglone (*1*) and its derivatives (*2*–*9*)

The MTT analysis showed that all compounds (**1–9**) exhibited cytotoxic activity against all tested cancer cell lines. Based on data collected from two independent experiments in triplicate, the IC_{50} values ranged from 1.7 to over 28.7 μM between cells after 72 h of incubation (Table 1). Compound **3** was the most active among all, with IC_{50} ranging from 1.7 to 4.7 μM in HL-60 and SF-295, respectively, whereas for the prototype (compound **1**), IC_{50} ranged from 7.6 to over 28.7 μM in HCT-8 and HL-60 and/or MDA-MB435, respectively. For normal PBMC, IC_{50} values for compounds **1** and **3** were over 28.7 and 3.7 μM, respectively. Compound **3** was, in fact, generally more active than compound **1** for all tested cells, including normal ones. While compound **3** was active more than 20 times in HL-60 cells, it was only 1.56 times more active against HCT-8 cells. Additionally, the selectively was hardly affected, since compound **3** was even more active to PMBC than to adherent tumor cells (HCT-8, MDA-MB-435 and SF-295).

Based on these results, all subsequent experiments were conducted to compare the cytotoxicity of juglone (compound **1**) and 5-methoxy-1,4-naphthoquinone (compound **3**) on the HL-60 cell line.

3.2. Morphological changes and cell death pattern induced by juglone (*1*) and its 5-*O*-methyl derivative (*3*)

Analysis by light microscopy of treated and untreated HL-60 cells revealed several drug-induced morphological changes. Control cells exhibited a typical non-adherent and vacuolization round morphology after 24 h in culture (Fig. 2 A). Juglone (**1**) at 4 μM

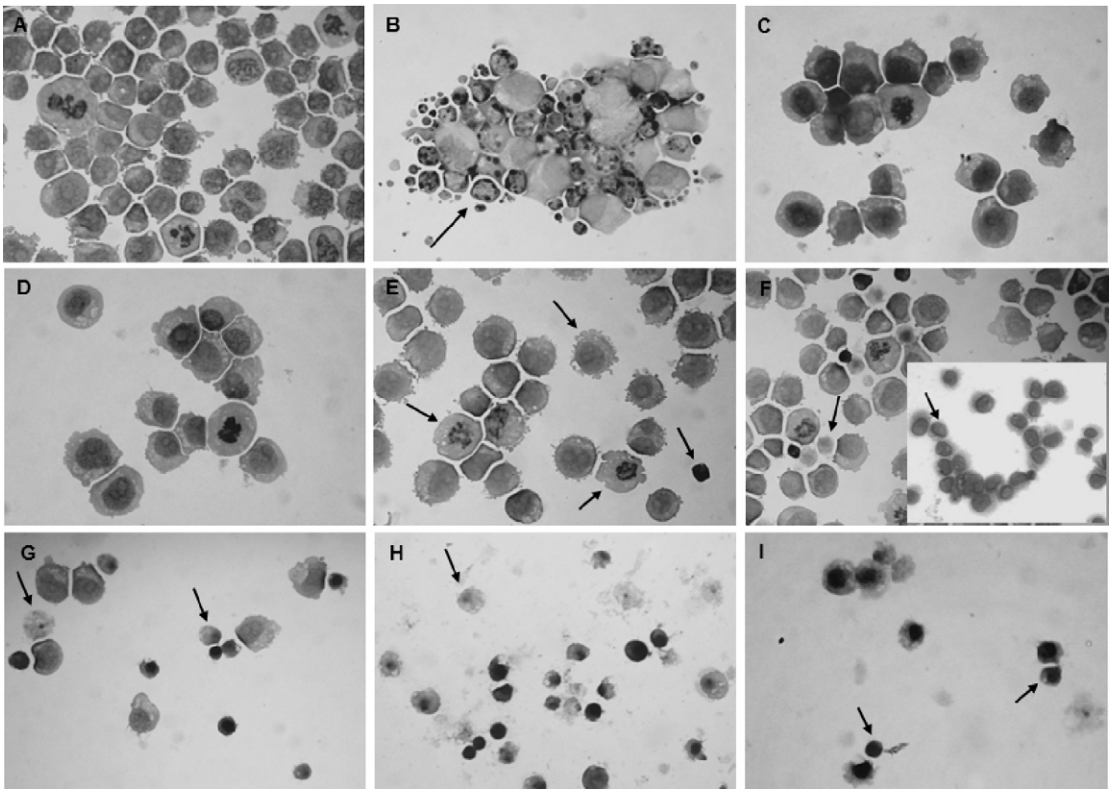

Fig. 2. Microscopic analysis of hematoxylin/eosin-stained. HL-60 cells untreated (**A**) or treated with compound **1** (4 μM, **C**) and compound **3** (0.5 μM, **D**, 1 μM, **E**, 2 μM, **F**, 4 μM, **G**, 8 μM, **H** or 10 μM, **I**) were analyzed by light microscopy (400×). Doxorubicin (0.5 μM) was used as positive control (**B**). At 2 μM (**F**) cells stained with May-Grunwald-Giemsa demonstrated chromatin condensation. Black arrows show smaller cells with intact membranes.

did not induce any noticeable changes in treated cells (Fig. 2C). On the other hand, HL-60 cells treated with **3** showed intense chromatin condensation, internuclear vacuoles, cytoplasm protuberances, reduction of the cell and nuclear volume, chromatolysis that became more evident for incubations at higher concentrations (Fig. 2E–I). Despite these typical apoptotic features, it was also observed an increasing number of cells with round shape, suggesting a preserved membrane, but smaller than a viable cell and with an intense staining, different from the viable ones (Fig. 2E–I) which were considered apoptotic cells. Doxorubicin (0.5 μM) induced cell shrinkage, chromatin condensation and nuclear fragmentation, on HL-60 cells, being all them, features of apoptosis (Fig. 2B).

Fluorescence microscopy confirmed the results found by light microscopy. After 24 h, HL-60 treated with **3** showed a decrease in cell viability in a dose-dependent manner, while the number of apoptotic cells increased with the concentration of compound **3,** corroborating the results reported above (Fig. 3). At the concentration of 1 and 2 μM of compound **3**, the viable cells were reduced by

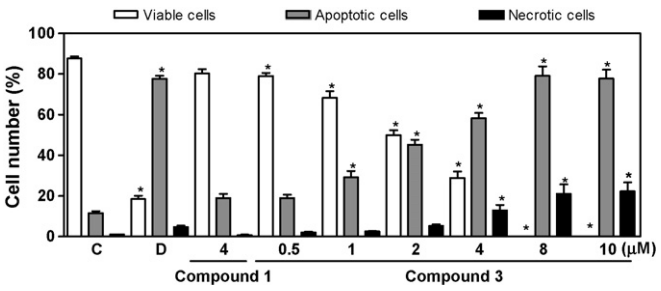

Fig. 3. Effects of compounds **1** and **3**, in HL-60 cell viability by acridine orange and ethidium bromide-stained (AO/EB) determined fluorescence microscope, after 24 h incubation. The negative control (**C**) was the vehicle used for diluting the tested substances. Doxorubicin (0.5 μM) was used as positive control (**D**). $^{*}p < 0.05$ compared to control by ANOVA, followed by Newman–Keuls multiple comparison test. Data are presented as mean values ± S.E.M. from three independent experiments performed in duplicate ($n = 6$).

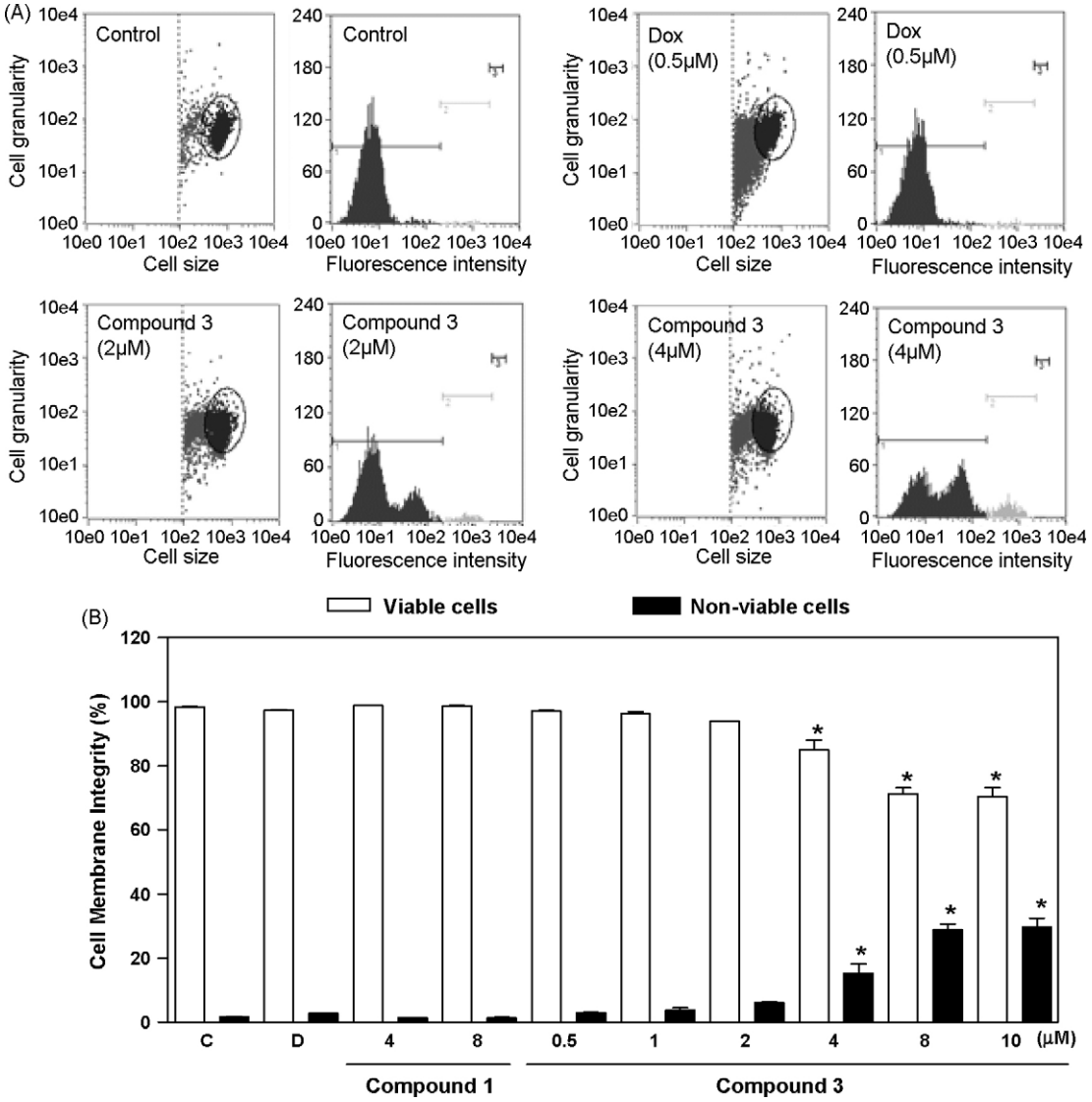

Fig. 4. Effects of juglone (**1**) and its 5-O-methyl derivative (**3**) at 2 and 4 μM in HL-60 cell population determined by flow cytometry using propidium iodide, after 24 h incubation. The negative control (**C**) was the vehicle used for diluting the tested substances. Doxorubicin (D) (0.5 μM) was used as a positive control. (**A**) The forward light scatter and side light scatter of the laser were used as indices of cell size and granularity, respectively. (**B**) Bars correspond to the means ± SEM of the percentage of viable and non-viable cells obtained from 3 independent experiments. Five thousand events were analyzed in each experiment. $^{*}p < 0.05$ compared to control by ANOVA, followed by Newman–Keuls multiple comparison test.

19.3% and 37.7%, respectively, followed by a significant reduction of 58.7% at 4 μM. No viable cells were observed at 8 or 10 μM, only the apoptotic and necrotic cells previously described. Also, apoptosis starts to occur, significantly, as early as 1 μM (29.1%) and it rises until 10 μM (77.7%). In respect to necrosis, it was shown a discrete increase in a dose-dependent manner, beginning at 4 μM (12.93%) following by 8 and 10 μM (12.9; 21% and 22.2%, respectively). No difference was observed after treatment with compound **1** at 4 μM and the negative control.

HL-60 cells treated for 24 h with **3** showed a decrease on cell size and granularity in a dose-dependent manner as observed by forward scatter and side scatter, respectively, but the membrane integrity was essentially preserved (Fig. 4A), confirming the previous results described above. Disruption of membrane integrity was observed only at concentrations equal or above 4 μM (Fig. 4B). No difference was observed for doxorubicin or compound **1** when compared with the negative control.

3.3. DNA fragmentation, cell cycle, PS externalization, mitochondrial depolarization and caspases activity

Since morphological changes indicated that treated cells are undergoing a possible apoptotic process, DNA fragmentation, PS externalization, mitochondrial depolarization and caspases activation were analyzed. The percentage of HL-60 cells with DNA fragmentation was significantly increased by the treatment with **3** as early as 2 μM (21.29%) ($p < 0.05$), in a dose-dependent manner, while no difference was observed for **1** at 4 μM (Fig. 5). Doxorubicin at 0.5 μM, used as a positive control, induced 54.14% of DNA fragmentation, comparable with data from compound **3** at 8 and 10 μM (68.10% and 70.68%, respectively). No cell cycle changes were observed (data not shown).

Based on PS externalization analysis, it can be demonstrated that compound **3,** at all tested concentrations, induces significant apoptosis. At the highest tested concentration (8 μM), 40.27% of treated cells presented initial apoptotic features, while 52.78% could be classified in the late apoptosis state (Fig. 6). Since all previous results indicate that compound **3** induces cell death by apoptosis, the pathway (intrinsic or extrinsic) triggering apoptosis was evaluated. Except for compound **3** at 10 μM (12.57% depolarization), no mitochondrial depolarization was observed for compound **1** and **3**, at all tested concentrations, while doxorubicin showed 51.27% of mitochondrial depolarization (Fig. 7). Activation of caspases 8 and 3/7 was also evaluated. The results showed that 66.07% and 82.57% of caspase 8 was activated at both concentrations tested (4 and 8 μM, respectively) (Fig. 8A) and 53.36% and 74.02% of caspase 3/7 was activated (Fig. 8B). All results presented herein, suggest that compound **3** induces apoptosis independent of mitochondria depolarization.

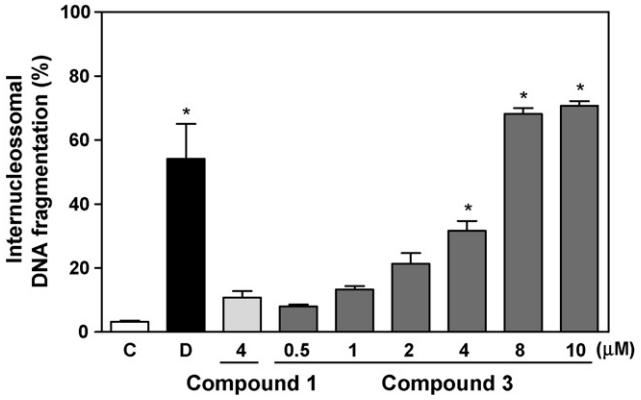

Fig. 5. Effects of compounds **1** and **3** in internucleosomal DNA fragmentation in HL-60 cells determined by flow cytometry using propidium iodide, Triton X-100 and citrate after 24 h incubation. The negative control (C) was the vehicle used for diluting the tested substance. Doxorubicin (0.5 μM) was used as positive control (D). Data are presented as mean values ± S.E.M. from three independent experiments performed in triplicate. Five thousand events were analyzed in each experiment. *$p < 0.01$ compared to control by ANOVA, followed by Newman–Keuls multiple comparison test.

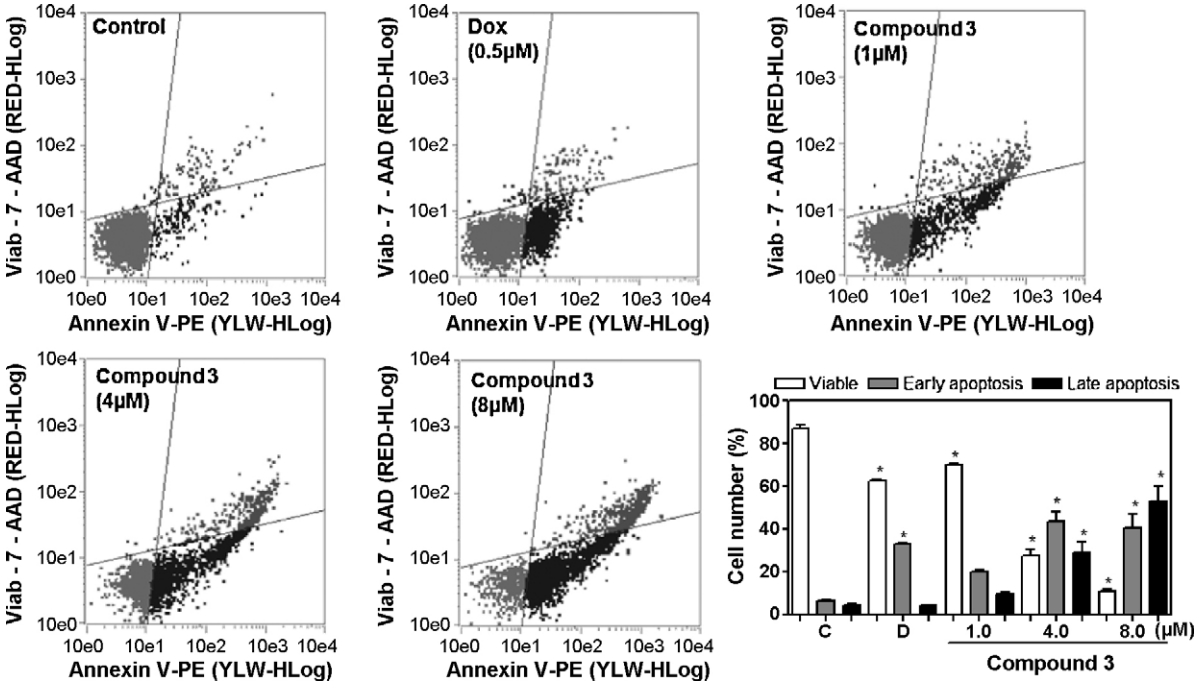

Fig. 6. Effects of compound **3** at 1 μM (**C**), 4 μM (**D**) and 8 μM (**E**) in HL-60 PS externalization determined by flow cytometry, using Annexin V-PE and 7-AAD after 24 h incubation. The negative control (**C**) was the vehicle used for diluting the tested substance. Doxorubicin at 0.5 μM was used as positive control (**D**). Data are presented as dot plot in which cell membrane integrity (7-AAD-*y*-axis) is plotted against PS externalization (Annexin V-PE-*x*-axis). Percentages of cells in early and late apoptosis and necrosis are indicated.

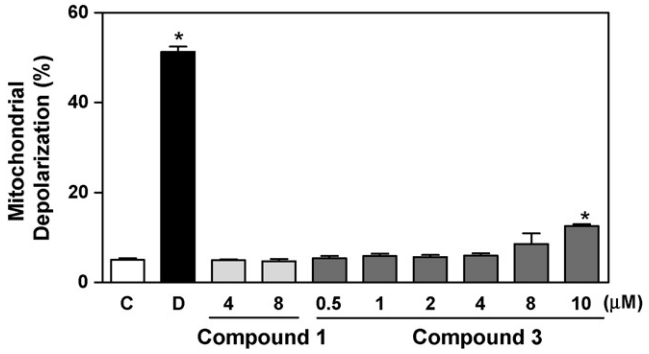

Fig. 7. Effects of compound **1** (4 and 8 μM, respectively) and compound **3** (0.5, 1, 2, 4, 8 and 10 μM) in HL-60 mitochondrial membrane depolarization, determined by flow cytometry using rhodamine123 after 24 h incubation. Negative control (C) was treated with the vehicle used for diluting the tested substance. Doxorubicin (0.5 μM) was used as positive control (D). Data are presented as histograms in which the cell number (*y*-axis) is plotted against cell membrane integrity (*x*-axis). Percentages of cells with mitochondrial membrane depolarization are indicated at each histogram.

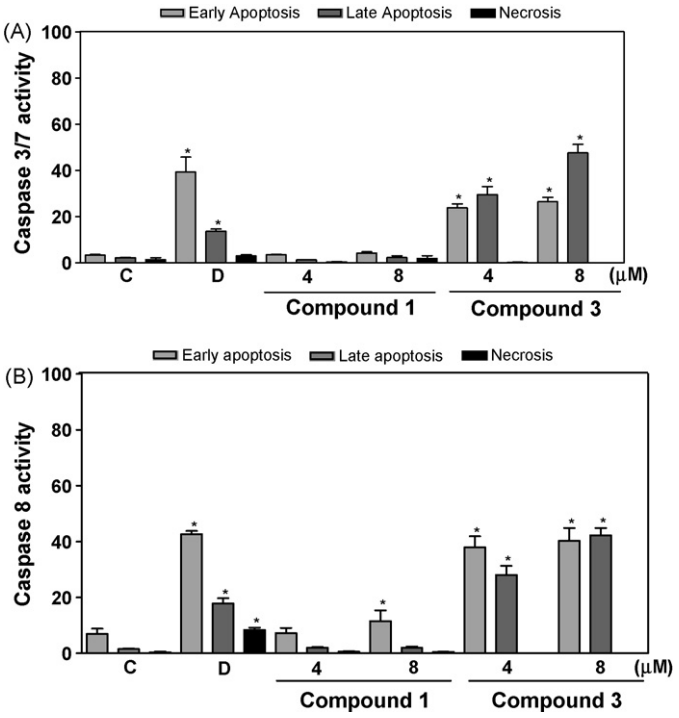

Fig. 8. Effects of compounds **1** and **3** in HL-60 caspase 3/7 (A) and caspase 8 (B) activity, determined by flow cytometry after 24 h incubation. Negative control (C) was treated with the vehicle used for diluting the tested substances. Doxorubicin (0.5 μM) was used as positive control (D). Data are presented as mean values ± S.E.M. from three independent experiments performed in triplicate. Five thousand events were analyzed in each experiment. $^{*}p < 0.01$ compared to control by ANOVA, followed by Student–Newman–Keuls test.

4. Discussion

The quinone moiety is present in many anticancer drugs such as anthracyclines (daunorubicin, doxorubicin), mitomycin and mitoxantrone, which are used clinically in the therapy of solid tumors [1]. In structural terms, the nine compounds tested can be divided into two series, depending on the absence (**I**, **1**–**3**) or presence of the bromo-substituent (**II**, **4**-**9**) in their structures. In **II**, they can be classified in **IIA** (2-bromo-substituted) and **IIB** (3-bromo-substituted). Comparing with juglone (**1**), the prototype, all the compounds (**2**–**9**), showed higher toxicity except for HCT-8 (colon cancer), for which juglone presented its higher activity (7.6 μM) (Table 1). In series **I**, methylation of juglone, furnishing **3**, led to a significant increase of activity toward all cell lines. The acetyl derivative **2** was also more active than juglone but less than juglone methyl ether **3**. Previous studies by Phillips [41] in a set of cancer cell lines, demonstrated that 1,4-naphthoquinone presented IC_{50} range from 0.6 to 690.4 μM in HT-29 (colon cancer) and H-460 (lung cancer), respectively. In the same study, 5-methoxy-1,4-naphthoquinone presented IC_{50} ranged from 2.5 to 12.9 μM in A459 and H460 (lung cancer), respectively.

With the introduction of a bromo-atom in position 2 or 3 on the juglone (**1** vs. **4** vs. **7**, Table 1), the IC_{50} significantly decreased, regardless the position on the NQ moiety. Comparing the methyl and acetyl derivatives (**2** vs. **5** vs. **8**), there is some similarity. Comparing **3**, **6** and **9**, the presence of bromo was ineffective, removing the original activity. In the series **IIA** (**4** vs. **5** vs. **6**), the –OH group is the most active, except for SF295 (similar activity) and HCT-8, whereas **5** presented a lower IC_{50}. In **IIB** (**7** vs. **8** vs. **9**), the methoxy **9** is more active, but still less active than **3**. Concerning to PBMC, compound **1** showed IC_{50} over 28 μM whereas for compound **3**, the IC_{50} was 3.7 μM, which could suggest an increase in the unspecific mechanisms of cytotoxicity. The selectivity index, obtained as the ratio between the IC_{50} (μM) value against PBMC and different cancer cell lines, ranged from ≅1 (PBMC vs. HL-60 and PBMC vs. MDA-MB-435) to 3.77 (PBMC vs. SF-295) for compound **1**, and from 0.78 (PBMC vs. SF-295) to 2.17 (PBMC vs. HL-60) for compound **3**. These data suggested that compound **3** presented a low selectivity to cancer cells.

Several studies have been performed to elucidate the mechanism of action of juglone (**1**) and it is well known that juglone exerts its effects by modifying sulphidryl groups [42] inhibiting different kinds of enzymes. In 2001, Chao et al. [43] demonstrated that juglone is an effective and rapid inhibitor of RNA polymerase II transcription and that juglone treatment causes cells to be refractory to lysis during stimuli. However, several studies demonstrated that juglone can induce apoptosis and/or necrosis, depending on dose-treatment [8,16,44]. Interestingly, compound **3** leads to severe morphological changes, markedly characterized by smaller cells and intrinsic fluorescence, which could be related to the refractoriness of membrane to lysis, keeping cell integrity even in the late stages of apoptosis process. In spite of these alterations, treated cells also presented morphological characteristics of apoptotic cells, such as chromatin condensation, a reduction in cell volume and fragmentation of the nuclei. Some authors consider the distinction between apoptosis and necrosis difficult and controversial, and the morphological definition of apoptosis and necrosis could be based on membrane integrity [45]. According to Dartsch et al. [46], there are two crucial points for the distinction between apoptosis and necrosis: the former is characterized by the occurrence of DNA and nuclear fragmentation with concomitant maintenance of membrane integrity and involves the triggering of phagocytic elimination of apoptotic bodies by the externalization of phosphatidyl serine. Our data are in agreement with this definition, since compound **3** leads to DNA fragmentation without affecting membrane integrity, and also induces phosphatidyl serine externalization.

The two major apoptosis signaling pathways in mammalian systems are the “extrinsic” pathway initiated by activation of membrane-bound death receptors leading to cleavage of caspase [47] and the “intrinsic” pathway characterized by mitochondrial depolarization, release of cytochrome c, and subsequent activation of caspases [48,49]. Thus, mitochondrial depolarization and the type of activated caspase may indicate the pathway involved in apoptosis induction. Some naphthoquinones can induce apoptosis via caspase activation [44,50]. In a study by Li and co-workers [44] it was demonstrated that a benzobijuglone induces apoptosis via activation of caspases 8 and 3. Our results corroborates those

of Li and co-workers [44]. HL-60 cells treated with compound **3** induce DNA fragmentation, activation of caspase 8 and 3/7 and lack of mitochondrial depolarization even in the higher dose, all known features of extrinsic apoptosis pathway, induced by death receptors that are at the cell surface. Also, apoptosis began as early as 0.5 μM with compound **3**, supporting all findings. It is clear that the receptors transmit apoptotic signals initiated by specific ligands and they play an important role in apoptosis activating the caspase cascade within seconds of ligand binding. Induction of apoptosis via this mechanism is therefore very rapid [51].

Death receptors have been proposed as a potential target for cancer therapy. They can be activated and induce tumor cell to commit apoptotic suicide independently of tumor suppressor p53 being useful in tumors that have lost p53 function. Targeting the death receptors in tumor cells might be a useful tool in cancer therapy, especially in tumors that have been resistant to conventional therapy [52]. Interestingly, HL-60 cell, the model used in this work, lacks p53 [53] and this cell line was the most sensitive to compound **3**.

In conclusion, the results presented herein reaffirm the cytotoxicity of simple quinones and demonstrate that the introduction of a methoxy group at C-5, strongly increases the cytotoxicity of juglone. Moreover, it was demonstrated that 5-methoxy-1,4-naphthoquinone induces apoptosis by an extrinsic pathway, and is, thus, independent of mitochondrial depolarization.

Conflict of interest statement

No conflict of interest.

Acknowledgments

We wish to thank CNPq, CSIC-CNPq (2005 BR0046, to M.T.M and M.O.F.G), DGICYT (Spain, grant BQU2003-00813 and SAF2006-04698 to M.T.M.)), CSIC (for a I3P contract, to E.L.-M.), CAPES, FUNCAP, FINEP, BNB/FUNDECI, FAPEAL, MCT/DECIT, MCT/MS/Neoplasias, IM-INOFAR/CNPq and PRONEX/FAPEAL for financial support in the form of grants and fellowship awards. We are grateful to Silvana França dos Santos and Luciana França for technical assistance.

References

[1] W.O. Foye (Ed.), Cancer Chemotherapeutic Agents, American Chemical Society, Washington, D.C., 1995, pp. 205–239.
[2] C. Asche, Antitumor quinones, Mini Rev. Med. Chem. 5 (2005) 449–467.
[3] R. Boutros, V. Lobjois, B. Ducommun, CDC25 phosphatases in cancer cells: key players? Good targets? Nat. Rev. Cancer 7 (2007) 495–507.
[4] M.D. Garrett, P. Workman, Discovering novel chemotherapeutic drugs for the third millennium, Eur. J. Cancer 35 (1999) 2010–2030.
[5] F.H. Fry, C. Jacob, Sensor/effector drug design with potential relevance to cancer, Curr. Pharm. Des. 12 (2006) 4479–4499.
[6] E.N. da Silva Júnior, C.F. de Deus, B.C. Cavalcanti, C. Pessoa, L.V. Costa-Lotufo, R.C. Montenegro, M.O. de Moraes, M.C.F.R. Pinto, C.A. de Simone, V.F. Ferreira, M.O.F. Goulart, C.K.Z. Andrade, A.V. Pinto, 3-Arylamino and 3-alkoxy-nor-β-lapachone derivatives: synthesis and cytotoxicity against cancer cell lines, J. Med. Chem. 53 (2010) 504–508.
[7] H. Kamei, T. Koide, Y. Hashimoto, M. Hasegawa, Inhibition of cell growth in culture by quinones, Cancer Biother. Radiopharm. 13 (1998) 185–188.
[8] J.F. Rippmann, S. Hobbie, C. Daiber, B. Guilliard, M. Bauer, J. Birk, H. Nar, P. Garin-Chesa, W.J. Rettig, A. Schnapp, Phosphorylation-dependent proline isomerization catalyzed by Pin1 is essential for tumor cell survival and entry into mitosis, Cell Growth Differ. 11 (2000) 409–416.
[9] N. Cenas, S. Prast, H. Nivinskas, J. Sarlauskas, E.S.J. Arnér, Interactions of nitroaromatic compounds with the mammalian selenoprotein thioredoxin reductase and the relation to induction of apoptosis in human cancer cells, J. Biol. Chem. 281 (2006) 5593–5603.
[10] E. Dickancaité, N. Cenas, A. Kalvelyté, N. Serapiniené, Toxicity of daunorubicin and naphthoquinones to HL-60 cells: an involvement of oxidative stress, Biochem. Mol. Biol. Int. 41 (1997) 987–994.
[11] J. Segura-Aguilar, K. Jönsson, U. Tidefelt, C. Paul, The cytotoxic effects of 5-OH-1,4-naphthoquinone and 5,8-di-OH-1,4-naphthoquinone on doxorubicin-resistant human Leukemia cells (HL-60), Leuk. Res. 16 (1992) 631–637.
[12] P. Babula, V. Adam, R. Kizek, Z. Sladky, L. Havel, Naphthoquinones as allelochemical triggers of programmed cell death, Environ. Exp. Bot. 65 (2009) 330–337.
[13] S. Sugie, K. Okamoto, K.M.W. Rahman, T. Tanaka, K. Kawai, J. Yamahara, H. Mori, Inhibitory effects of plumbagin and juglone on azoxymethane-induced intestinal carcinogenesis in rats, Cancer Lett. 127 (1998) 177–183.
[14] M.T. Paulsen, M. Ljungman, The natural toxin juglone causes degradation of p53 and induces rapid H2AX phosphorylation and cell death in human fibroblasts, Toxicol. Applied Pharmacol. 209 (2005) 1–9.
[15] S.K. Sandur, H. Ichikawa, G. Sethi, K.S. Ahn, B.B. Aggarwal, Plumbagin (5-hydroxy-2-methyl-1,4-naphthoquinone) suppresses NF-κB activation and NF-κB-regulated gene products through modulation of p65 and Iκ Bα kinase activation, leading to potentiation of apoptosis induced by cytokine and chemotherapeutic agents, J. Biol. Chem. 281 (2006) 17023–17033.
[16] B.K. Aithal, M.R.S. Kumar, B.N. Rao, N. Udupa, B.S.S. Rao, Juglone, a naphthoquinone from walnut, exerts cytotoxic and genotoxic effects against cultured melanoma tumor cells, Cell Biol. Int. 33 (2009) 1039–1049.
[17] K. Krohn, N. Böker, 1,2-, 1,4-, 2,9- and 9,0-anthraquinones and higher fused polycyclic quinone derivatives, in: A.G. Griesbeck (Ed.), Science in Synthesis, Thieme Verlag, Stuttagart, 2006, pp. 367–506.
[18] M.C. Carreño, A. Urbano, Recent advances in the synthesis of angucyclines, Synlett 1 (2005) 1–25.
[19] J.A. Valderrama, M.F. González, C. Valderrama, Studies on quinones. Part 32. Regioselective synthesis of benz[b]phenantridines related to phenantroviridone, Tetrahedron 55 (1999) 6039–6050.
[20] K.A.L. Ribeiro, C.M. de Carvalho, M.T. Molina, E.P. Lima, E. López-Montero, J.R.M. Reys, M.B.F. de Oliveira, A.V. Pinto, A.E.G. Santana, M.O.F. Goulart, Activities of naphthoquinones against *Aedes aegypti*, vector of dengue and *Biomphalaria glabrata*, intermediate host of *Schistosoma mansoni*, Acta Trop. 111 (2009) 44–50.
[21] L.F. Tietze, C. Güntner, K.M. Gericke, A Diels-Alder reaction for the total synthesis of the novel antibiotic antitumor agent mensacarcin, Eur. J. Org. Chem. (2005) 2459–2467.
[22] M.P. Sibi, J.W. Dankwardt, V. Snieckus, Anionic aromatic ring annelation of o-allylbenzamides. Regiospecific synthesis of naphthols and naphthoquinones, J. Org. Chem. 51 (1986) 271–273.
[23] L.F. Fieser, J.T. Dunn, Addition of dienes to halogenated and hydroxylated naphthoquinones, J. Am. Chem. Soc. 59 (1937) 1016–1021.
[24] J.H. Bowie, D.W. Cameron, D.H. Williams, Studies in mass spectrometry. I. Mass spectra of substituted naphthoquinones, J. Am. Chem. Soc. 87 (1965) 5094–5099.
[25] R.L. Hannan, R.B. Barber, H. Rapoport, Synthesis of bromonaphthoquinones from 1,3-dimethoxynaphthalene, J. Org. Chem. 44 (1979) 2153–2158.
[26] J.F. Garden, R.H. Thomson, Quinones. Part VI. Some new polyhydroxynaphthoquinones, J. Chem. Soc. (1957) 2483–2489.
[27] J.R. Grunwell, A. Karipides, C.T. Wigal, S.W. Heinzman, J. Parlow, J.A. Surso, L. Clayton, F.J. Fleitz, M. Daffner, J.E. Stevens, The formal oxidative addition of electron-rich transoid dienes to bromonaphthoquinones, J. Org. Chem. 56 (1991) 91–95.
[28] M.A. Brimble, T.J. Brenstrum, C-Glycosylation of tri-O-benzyl-2-deoxy-D-glucose: synthesis of naphthyl substituted 3,6-dioxabicyclo[3.2.2]nonanes, J. Chem. Soc. [Perkin 1] (2001) 1612–1623.
[29] R.H. Thomson, Studies in the juglone series. I. Some halogen derivatives and their reaction with aniline, J. Org. Chem. 13 (1948) 377–383.
[30] K.A. Parker, M.E. Sworin, Assignment of regiochemistry to substituted naphthoquinones by bromo juglone derivatives chemical and spectroscopic methods amino-, hydroxy-, and bromojuglone derivatives, J. Org. Chem. 46 (1981) 3218–3223.
[31] M.E. Jung, J.A. Hagenah, Synthetic approach to aklavinone using 2-oxo-2H-pyran-5-carboxylate (coumalate) intermediates, J. Org. Chem. 52 (1987) 1889–1902.
[32] A.M. Echavarren, N. Tamayo, O. de Frutos, A. Garcia, Synthesis of benzo[b]carbazoloquinones by coupling of organostannanes with bromoquinones, Tetrahedron 53 (1997) 16835–16846.
[33] L.F. Tietze, K.M. Gericke, I. Schuberth, Synthesis of highly functionalized anthraquinones and evaluation of their antitumor activity, Eur. J. Org. Chem. (2007) 4563–4577.
[34] M.T. Molina, C. Navarro, A. Moreno, A.G. Csaky, Arylation of benzo-fused 1,4-quinones by the addition of boronic acids under dicationic Pd(II)-catalysis, Org. Lett. 11 (2009) 4938–4941.
[35] T.J. Mosmann, Rapid colorimetric assay for cellular growth and survivor: application to proliferation and cytotoxicity assays, J. Immunol. Methods 65 (1983) 55–63.
[36] S.A. Ahmed, R.M. Gogal, J.E. Walsh, A new rapid and simple non-radioactive assay to monitor and determine the proliferation of lymphocytes an alternative to [3H]thymidine incorporation assay, J. Immunol. Methods 170 (1994) 211–224.
[37] M.F. Cury-Boaventura, C. Pompeia, R. Curi, Comparative toxicity of oleic acid and linoleic acid on Jurkat cells, Clin. Nutr. 23 (2004) 721–732.
[38] Z. Darzynkiewicz, S. Bruno, G. Del Bino, W. Gorczyca, M.A. Hotz, P. Lassota, F. Traganos, Features of apoptotic cells measured by flow cytometry, Cytometry 13 (1992) 795–808.
[39] I. Nicoletti, G. Migliorati, M.C. Pagliacci, F. Grignani, C. Riccardi, A rapid and simple method for measuring thymocyte apoptosis by propidium iodide staining and flow cytometry, J. Immunol. Methods 139 (1991) 271–279.

[40] I. Vermes, C. Haanen, H. Steffens-Nakken, C. Reutelingsperger, A novel assay for apoptosis. Flow cytometric detection of phosphatidylserine expression on early apoptotic cells using fluorescein labelled Annexin V, J. Immunol. Methods 184 (1995) 39–51.
[41] R.M. Phillips, M. Jaffar, D.J. Maitland, P.M. Loadman, S.D. Shnyder, G. Steans, P.A. Cooper, A. Race, A.V. Patterson, I.J. Stratford, Pharmacological and biological evaluation of a series of substituted 1,4-naphthoquinone bioreductive drugs, Biochem. Pharmacol. 68 (2004) 2107–2116.
[42] L. Henning, C. Christner, M. Kipping, B. Schelbert, K.P. Rucknagel, S. Grabley, G. Kullertz, G. Fischer, Selective inactivation of parvulin-like peptidyl-prolyl cis/trans isomerases by juglone, Biochemistry 37 (1998) 5953–5960.
[43] S.H. Chao, A.L. Greenleaf, D.H. Price, Juglone, an inhibitor of the peptidyl-prolyl isomerase Pin1, also directly blocks transcription, Nucl. Acids Res. 29 (2001) 767–773.
[44] Z.B. Li, J.Y. Wang, B. Jiang, X.L. Zhang, L.J. An, Y.M. Bao, Benzobijuglone, a novel cytotoxic compound from *Juglans mandshurica*, induced apoptosis in HeLa cervical cancer cells, Phytomedicine 14 (2007) 846–852.
[45] M. Masquelier, Q.F. Zhou, A. Gruber, S. Vitols, Relationship between daunorubicin concentration and apoptosis induction in leukemic cells, Biochem. Pharmacology 67 (2004) 1047–1056.
[46] D.C. Dartsch, A. Schaefer, S. Boldt, W. Kolch, H. Marquardt, Comparison of anthracycline-induced death of human leukemia cells: programmed cell death versus necrosis, Apoptosis 7 (2002) 537–548.
[47] A. Ashkenazi, V.M. Dixit, Death receptors: signaling and modulation, Science 281 (1998) 1305–1308.
[48] D.R. Green, J.C. Reed, Mitochondria and apoptosis, Science 281 (1998) 1309–1312.
[49] R. Khosravi-Far, M.D. Esposti, Death receptor signals to mitochondria, Cancer Biol. Ther. 3 (2004) 1051–1057.
[50] K.H. Kang, K.H. Lee, M.Y. Kim, K.H. Choi, Caspase-3-mediated cleavage of the NF-κB subunit p65 at the NH_2 terminus potentiates naphthoquinone analog-induced apoptosis, J. Biol. Chem. 276 (2001) 24638–24644.
[51] I.M. Ghobrial, T.E. Witzig, A.A. Adjei, Targeting apoptosis pathways in cancer therapy, Cancer J. Clin. 55 (2005) 178–194.
[52] H.N. LeBlanc, A. Ashkenazi, Apo2L/TRAIL and its death and decay receptors, Cell Death Differ. 10 (2003) 66–75.
[53] H. Berglind, Y. Pawitan, S. Kato, C. Ishioka, T. Soussi, Analysis of p53 mutation status in human cancer cell lines, Cancer Biol. Ther. 7 (2008) 701–710.